Discovery of 3-{5-[(6-Amino-1*H*-pyrazolo[3,4-*b*]pyridine-3-yl)methoxy]-2-chlorophenoxy}-5-chlorobenzonitrile (MK-4965): A Potent, Orally Bioavailable HIV-1 Non-Nucleoside Reverse Transcriptase Inhibitor with Improved Potency against Key Mutant Viruses

Thomas J. Tucker,*[,†] John T. Sisko,[†] Robert M. Tynebor,[†] Theresa M. Williams,[†] Peter J. Felock,[§] Jessica A. Flynn,[‡] Ming-Tain Lai,[§] Yuexia Liang,[#] Georgia McGaughey,[†] Meiquing Liu,[§] Mike Miller,[§] Gregory Moyer,[‡] Vandna Munshi,[§] Rebecca Perlow-Poehnelt,[†] Sridhar Prasad,[†] John C. Reid,[†] Rosa Sanchez,[#] Maricel Torrent,[†] Joseph P. Vacca,[†] Bang-Lin Wan,[†] and Youwei Yan[†]

Departments of Medicinal Chemistry and Structural Biology, Antiviral Research, Vaccines and Biologics Research, and Drug Metabolism, Merck Research Laboratories, WP14-3, 770 Sumneytown Pike, P.O. Box 4, West Point, Pennsylvania 19486-0004

Received July 11, 2008

Non-nucleoside reverse transcriptase inhibitors (NNRTIs) have been shown to be a key component of highly active antiretroviral therapy (HAART). The use of NNRTIs has become part of standard combination antiviral therapies producing clinical outcomes with efficacy comparable to other antiviral regimens. There is, however, a critical issue with the emergence of clinical resistance, and a need has arisen for novel NNRTIs with a broad spectrum of activity against key HIV-1 RT mutations. Using a combination of traditional medicinal chemistry/SAR analyses, crystallography, and molecular modeling, we have designed and synthesized a series of novel, highly potent NNRTIs that possess broad spectrum antiviral activity and good pharmacokinetic profiles. Further refinement of key compounds in this series to optimize physical properties and pharmacokinetics has resulted in the identification of **8e** (MK-4965), which has high levels of potency against wild-type and key mutant viruses, excellent oral bioavailability and overall pharmacokinetics, and a clean ancillary profile.

Introduction

Non-nucleoside reverse transcriptase inhibitors (NNRTIs[a]) are a key component of highly active antiretroviral therapy (HAART). NNRTIs target an allosteric binding pocket on the reverse transcriptase enzyme, and their binding is noncompetitive with respect to dNTPs and template/primer.[1] There are currently three commercially available first generation NNRTIs: efavirenz, nevirapine, and delavirdine (Figure 1).[2] Despite the demonstrated clinical efficacy of these compounds, the emergence of clinical resistance has become a key issue and a major cause of treatment failure. Recently, the second generation NNRTI etravirine (TMC-125, Figure 1) has been approved by the FDA and has demonstrated activity toward a number of clinically observed mutations.[3] However, the need remains for alternative second generation NNRTIs that have a broad spectrum of activity versus mutant viruses and a high genetic barrier to the selection of new resistant strains. Since compliance is also a key issue in anti-HIV therapy, the need also exists for compounds that are safe, are easy to dose orally once a day, and have low potential for drug−drug interactions. Our efforts have focused on the design and synthesis of novel NNRTIs with potent and broad spectrum mutant activity that are also safe and have pharmacokinetics suitable for once a day oral dosing.

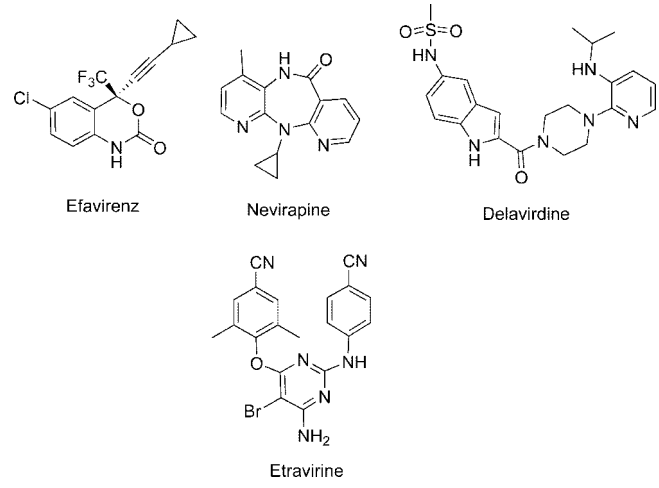

Figure 1. Currently marketed NNRTIs.

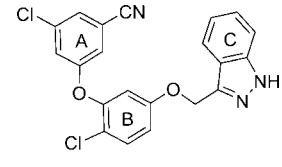

Figure 2

In a previous manuscript, we described our early efforts toward the design and synthesis of novel second generation NNRTIs and presented a potent and novel diaryl ether/indazole template **1** (Figure 2).[4] Compound **1** possesses potent antiviral activity versus WT and a variety of clinically relevant mutant viruses.[4] Unfortunately, **1** has low solubility and low oral

* To whom correspondence should be addressed. Phone: 1-215-652-5275. Fax: 1-215-652-3971. E-mail: tom_tucker@merck.com.
† Department of Medicinal Chemistry and Structural Biology.
§ Department of Antiviral Research.
‡ Department of Vaccines and Biologics Research.
# Department of Drug Metabolism.

[a] Abbreviations: NNRTI, non-nucleoside reverse transcriptase inhibitor; HAART, highly active antiretroviral therapy; WT, wild type; CIC_{95}, cell inhibitory concentration that blocks 95% of viral replication; FBS, fetal bovine serum; NHS, normal human serum; MOI, multiple of infection.

10.1021/jm800856c CCC: $40.75
Published on Web 10/01/2008

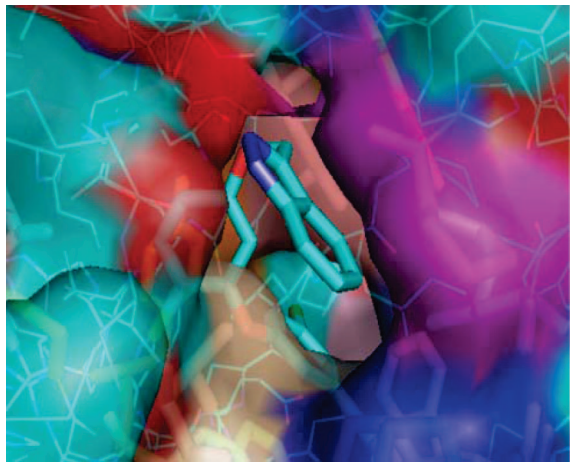

Figure 3. X-ray crystal structure of **1** bound in WT NNRTI binding site (from ref 4). View is looking inward along the enzyme−solvent interface under P236 (magenta), showing the solvent exposed lower surface of the indazole C ring.

bioavailability that precluded its further development. Further efforts in this series have focused on preparing more soluble versions of **1** that we hypothesized would have better overall physical properties and improved pharmacokinetic profiles after oral dosing. Crystallographic studies with **1**[4] showed that the lower edge of the indazole C ring lies under the P236 residue along the enzyme/solvent interface (Figure 3), and as such, we hypothesized that this region should be amenable to functionalization with polar, solubilizing substituents. We proposed to prepare a number of analogues of **1** in which the phenyl ring of the indazole moiety was replaced with a pyridine ring, with the goal of finding a close derivative that showed enhanced solubility and oral bioavailability while retaining the desirable overall biological profile seen with **1**. In this manuscript, we describe the design, synthesis, and biological profile of this series of pyridine analogues that has led to the discovery of novel NNRTIs suitable for clinical development.

Chemistry

Target compounds were prepared by the generic method shown in Scheme 1. S_NAr reaction of phenol **2** and aryl fluoride **3** provided the protected diaryl ether intermediate **4** in good yield. Removal of the methyl protecting group with boron tribromide progressed in excellent yield to give the key phenol intermediate **5**. The target compounds were then prepared in a two-step sequence via alkylation of the phenol **5** with the 1-Boc-3-bromomethylpyrazolopyridines **6a**−**d**, followed by removal of the Boc protecting group with TFA to give the target compounds **8a**−**d**. The critical bromo intermediates **6a**[5] and **6d**[5] were prepared via literature methods; however, bromides **6b** and **6c** were not known in the literature and were prepared by modification of related literature methodologies[6,7] as detailed in Scheme 2. Ortho directed metalation of 4-chloropyridine **9** and reaction with the Weinreb amide provided the ketone intermediate **10**. Heating **10** with hydrazine in the presence ot titanium isopropoxide effected ring closure to the 3-methylpyrazolopyridine **11**. Compound **11** was protected selectively in the 1-position using standard conditions, and the protected intermediate **12** was brominated with NBS to provide the desired bromide **6b** in moderate yield. Bromide **6c** was synthesized in a similar manner, starting from 3-amino-4-methylpyridine **13**. Protection of the amino group using sodium hexamethyldisilazane and Boc anhydride gave the protected intermediate **14** in good yield. The methyl group in the 4-position was homologated to an ethyl group via directed metalation and treatment with iodomethane to give **15**. Removal of the Boc protecting group with TFA and subsequent diazotization/cyclization of the amino intermediate **16** yielded the 3-methylpyrazolopyridine derivative **17.** Compound **17** was converted to the desired bromide **6c** via a two-step protection/bromination as described above.

The 6-amino-7-aza derivative **8e** was synthesized using a strategy similar to that detailed above (Scheme 3). Ortho directed metalation of 2,6-difluoropyridine (**19**) and subsequent quenching with the requisite Weinreb amide gave the ketone **20** in modest yield. Numerous attempts to modify the conditions of this metalation failed to provide increased yields. The intermediate ketone **20** was treated with hydrazine in the presence of titanium isopropoxide to give the hydrazone intermediate, and the hydrazone was refluxed in ethanol to effect efficient cyclization to the 3-methyl-6-fluoropyrazolopyridine intermediate **21**. In a manner similar to that described previously for the des-fluoro analogues, **21** was Boc protected and brominated to give the bromide intermediate **23**. In a procedure similar to that described above (Scheme 1), alkylation of the phenol **5** with bromide **23** provided **24** in good yield. Displacement of the fluorine of **24** with PMB amine also removed the N1-Boc protecting group to provide the protected intermediate **25**. Heating **25** in neat TFA provided the desired target compound **8e** in good yield.

Results and Discussion

Table 1 details the in vitro biological data for efavirenz, **1**, and **8a**−**e**. Compounds were evaluated for intrinsic enzyme inhibitory potency versus WT RT (wild type HIV-1 reverse transcriptase), as well as the K103N and Y181C mutant RTs.[8] Compounds were also evaluated for antiviral potency (CIC_{95}) against WT and the key mutant viruses in the presence of 10% FBS (fetal bovine serum; WT and mutants) as well as 50% NHS (normal human serum; WT) to evaluate the effects of protein binding.[9] In general, inhibitory activity and antiviral activity improved as the nitrogen was moved around the aromatic ring from the 4-position (**8a**) to the 7-position (**8d**) in accord with our earlier hypothesis. The 7-aza analogue **8d** exhibited highly potent enzyme inhibitory activity versus WT and the key mutants and also showed excellent antiviral potency against the same panel. Pharmacokinetic studies with **8d** (Table 2) showed that the compound possessed promising pharmacokinetics after both iv and po dosing in several species, and as such, **8d** became a compound of high interest in our program. Crystallographic studies with **8d**[10] (Figure 4) demonstrate that the compound binds to the K103N mutant−NNRTI binding pocket in a manner analogous to that reported previously for **1** in the WT binding site. All of the key interactions of the western A ring and central B ring with the Y181C−Y188C−W229 lipophilic binding pocket are maintained as seen previously with the structure of **1** bound to the WT enzyme. The Y181 side chain is rotated by 90° as seen in previous crystal structures that we have reported in this series.[4] The two nitrogens of the pyrazolo moiety maintain two key hydrogen bonding interactions with the backbone carbonyl oxygen and NH of the K103 residue, and it is likely that this key interaction is critical for the high levels of potency observed versus the K103N mutant. The pyrazolopyridine heterocycle makes a stacking interaction with Y318 and also appears to make lipophilic interactions with the side chains of F227, P236, and V106. The bottom edge of this pyridyl ring lies along the enzyme−solvent interface as anticipated, and the nitrogen atom appears to be solvent exposed.

Scheme 1[a]

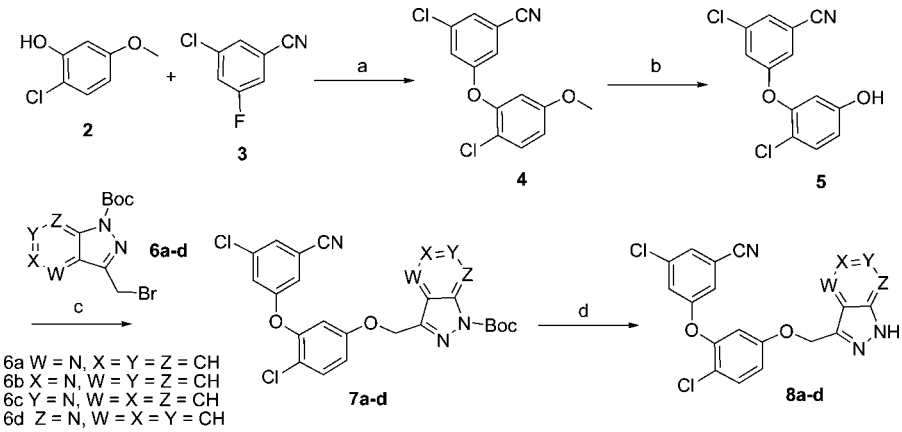

[a] Reagents: (a) K_2CO_3, NMP, 120 °C (75%); (b) BBr_3, CH_2Cl_2 (95%); (c) NaH or Cs_2CO_3, DMF; (d) TFA (10−80% for two steps).

Scheme 2. Synthesis of Bromides **6b** and **6c**[a]

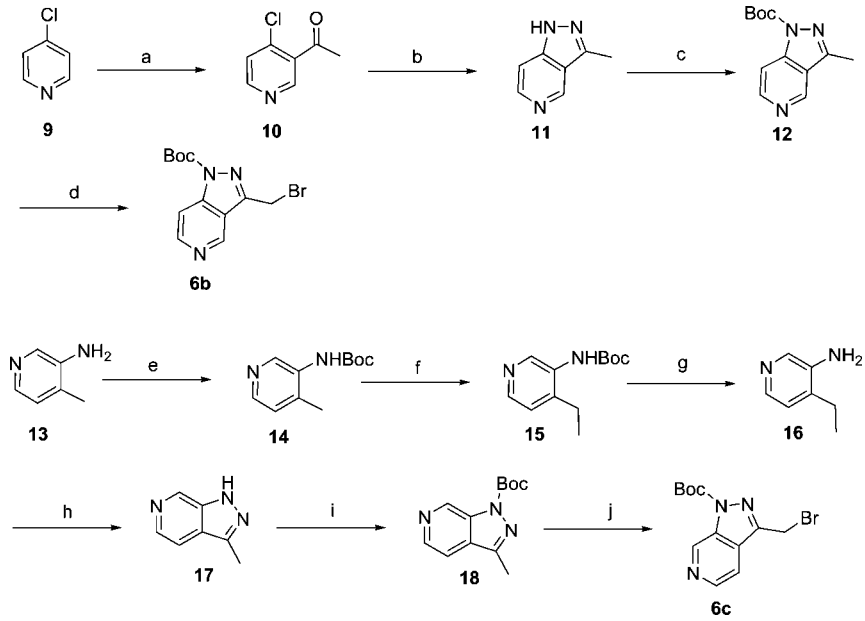

[a] Reagents: (a) LDA, *N*-methoxy-*N*-methylacetamide, THF, −78 °C (34%); (b) $Ti(iOPr)_4$, hydrazine hydrate, ethylene glycol, 120 °C (47%); (c) $(Boc)_2O$, DMAP, TEA, acetonitrile (67%); (d) NBS, benzoyl peroxide, CCl_4 (20%); (e) $Na(TMS)_2$, $(Boc)_2O$, THF (70%); (f) *t*-BuLi, CH_3I, THF (98%); (g) TFA (69%); (h) $NaNO_2$, 50% H_2SO_4 (51%); (i) $(Boc)_2O$, DMAP, TEA, acetonitrile (59%); (j) NBS, benzoyl peroxide, CCl_4, reflux (36%).

Further evaluation of **8d** versus a wider panel of clinically relevant mutant viruses[11] (Table 3) showed that the compound possessed broad activity versus most of the mutants tested. Only the Y188L mutation provided notable decreases in potency; this is presumably due to the direct interaction between the phenyl ring of **8d** and the aryl ring of the Y188 residue. When the residue is mutated to a leucine, much of the interaction between the phenyl ring and the side chain is lost because of the decreased size of the side chain as well as the loss of the π-stacking interaction. Y188L is a rare mutation, occurring in only 0.6% of clinical isolates.[12] The Y188L mutation requires a two-base change in its codon, indicating that progression to this mutation occurs in a stepwise manner via several intermediate mutations.[12] While the Y188L virus itself exhibits good fitness, the intermediate mutation Y188H is a much less fit virus, and the Y188F intermediate mutation appears to be slow growing.[12] In-house cell culture selection experiments with later members of this class have failed to select for the Y188L mutation under a variety of conditions (details of the data for the final development candidate will be presented later in this manuscript). While these studies suggest that the Y188L mutation may not be a serious issue for this series of compounds, it is also possible that secondary mutations could confer added fitness to one of the Y188L intermediates given the preexisting pool of viral mutations in a treatment experienced population. Therefore, only actual clinical experience with a compound of this class will provide a suitable answer to this question.

On the basis of its excellent overall profile, **8d** became a development candidate and was designated as MK-1107.[8] Full ancillary evaluation of **8d** showed the compound to be devoid of significant off-target activities, and the compound was also negative in preliminary genotoxicity determinations. Unfortunately, as **8d** was being studied in depth to support its further development, difficulty was encountered producing a formulation that could provide the high exposures necessary to support po dosing in these safety studies. Further in vivo studies showed that the compound was orally bioavailable only when dosed as a solution, and this became an issue given the low solubility of the compound especially as higher doses/exposures were needed. While **8d** did have improved solubility versus **1** (solubility of

Scheme 3[a]

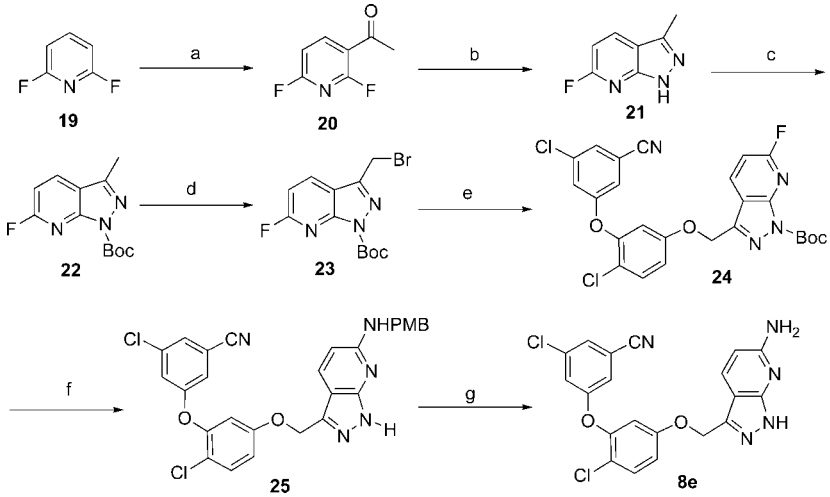

[a] Reagents: (a) LDA, *N*-methoxy-*N*-methylacetamide, THF, −78 °C (25%); (b) $Ti(iOPr)_4$, hydrazine hydrate, EtOH, reflux (95%); (c) $(Boc)_2O$, DMAP, TEA, acetonitrile (64%); (d) NBS, benzoyl peroxide, CCl_4, reflux (64%); (e) Cs_2CO_3, **5**, NMP (86%); (f) $PMBNH_2$, NMP, 95 °C (31%); (g) TFA, 60 °C (30%).

Table 1. Enzyme Inhibition and Antiviral Activity for Compounds **1** and **8a**−**e**

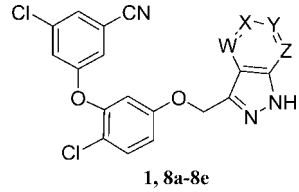

1, 8a-8e

					inhibition of RT polymerase, IC_{50} (nM)[a]			antiviral activity in cell culture, CIC_{95} (nM)[b]			
compd	W	X	Y	Z	WT	K103N	Y181C	WT (10% FBS)	K103N (10% FBS)	Y181C (10% FBS)	WT (50% NHS)
efavirenz					1.0	18.9	7.2	4.6	245	87	42
1	CH	CH	CH	CH	1.4 ± 0.3	1.1 ± 0.3	2.6 ± 0.4	22.6 ± 1.2	33 ± 1.9	102 ± 1.8	114 ± 1.7
8a	N	CH	CH	CH	3.6	40	740	307	2767	ND	922
8b	CH	N	CH	CH	1.2	3.8	6.2	169	922	278	307
8c	CH	CH	N	CH	0.8	1.3	3.9	10.8	34.2	31	34
8d	CH	CH	CH	N	0.4 ± 0.2	0.5 ± 0.2	0.2 ± 0.1	10.3 ± 1.1	14.6 ± 1.1	22 ± 1.2	34 ± 1.3
8e	CH	CH	C-NH_2	N	0.2 ± 0.1	0.5 ± 0.2	0.4 ± 0.2	8.4 ± 1.0	11.4 ± 1.1	19 ± 1.0	34 ± 1.1

[a] Compounds were evaluated in a standard SPA assay. For compounds **8a**−**c**, $n = 2$ and the values are the geometric mean of two determinations; all individual values are within 25% of the mean. For compound **1** where $n > 3$ and compounds **8d** and **8e** where $n > 50$, standard deviations are included. Assay protocols are detailed in ref 8. [b] CIC_{95} (cell culture inhibitory concentration) is defined as the concentration at which the spread of virus is inhibited by >95% in MT-4 human T-lymphoid cells maintained in RPMI 1640 medium containing either 10% FBS or 50% NHS. Details of the assay protocols are provided in ref 9. ND = not determined. For compounds **8a**−**c**, $n = 2$ and the values are the geometric mean of two determinations; all individual values are within 25% of the mean. For compound **1** where $n > 3$ and **8d** and **8e** where $n > 50$, standard deviations are included. No cytotoxicity was observed for any of the compounds up to the upper limit of the assay (8.3 μM).

8d at pH 7 is 0.1 μg/mL, while the solubility of **1** is so low that it cannot be determined), it appeared that further enhancements in solubility would be necessary to provide a compound whose exposure was not limited by solubility. As a result, development of the compound was halted, and we were forced to reevaluate our efforts in an attempt to further enhance the solubility and physical properties of this series. Once again, we sought to make minor changes to the structure of **8d** in an effort to retain the aforementioned excellent biological profile of the compound. Using **8d** as a starting point, we hypothesized that by adding an amino group in the 6-position of the pyridine ring, we could further enhance the basicity and possibly increase the solubility (especially at acidic pH) of this series of compounds while also maintaining the excellent overall profile of previous compounds in this series. A pyridyl nitrogen was reasonably well tolerated at the 6-position in a previous analogue in this series (Table 1, **8c**), suggesting that the introduction of an amino group at this position might also be well tolerated. Molecular modeling studies[13] suggested that this compound would be accommodated by the active site in a similar manner to **1** and **8d**, with the 6-amino group lying in the solvent exposed region and not making any detrimental interactions with the enzyme. Compound **8e** was synthesized (Scheme 3) and was shown to possess enzyme inhibitory activity and antiviral activity similar to that observed with **8d** (Table 1). **8e** was shown to be several orders of magnitude more soluble than **8d** especially at acidic pH (solubility of **8d** is <0.1 μg/mL at pH 2; solubility of **8e** is 10 μg/mL at pH 2), and these data encouraged further evaluation of the compound. Pharmacokinetic evaluation of **8e** (Table 2) demonstrated that this compound possessed a similar profile to **8d** in several species. More importantly, additional in vivo studies with **8e** showed that the compound was fully orally bioavailable in a dose proportional manner when dosed as either a suspension or a solution. Evaluation of **8e** (Table 3) against a wider panel of clinically relevant mutations confirmed that the compound retained excellent antiviral activity versus most

Table 2. Pharmacokinetic Parameters for **8d** and **8e** in Rat, Dog, and Rhesus

	8d			8e		
	rat[a]	dog[b]	rhesus[c]	rat[d]	dog[e]	rhesus[f]
$T_{1/2}$ (h)	4.1	11.8	8.2	3.5	3.9	2.1
Cl ((mL/min)/kg)	28	8.9	19	9	5.8	15.8
AUC_{po} (μM h)	9.5	1.6	0.3	22.7	31.3	0.3
V_d (L/kg)	5.3	2.6	4.4	2	1.7	1.9
F (%)	58	17	3	52	47	1

[a] Average of three Sprague−Dawley rats dosed at 10 mpk po (Imwitor/Tween) and 2 mpk iv (DMSO). All values are within 25% of the mean. [b] Average of two beagle dogs dosed at 2 mpk po (Imwitor/Tween) and 0.25 mpk iv (DMSO). [c] Average of two rhesus macaques dosed at 10 mpk po (Imwitor/Tween) and 1 mpk iv (DMSO). [d] Average of three Sprague−Dawley rats dosed at 10 mpk po (0.5% methocel) and 3 mpk iv (DMSO). All values are within 25% of the mean. [e] Average of three beagle dogs dosed at 10 mpk po (0.5% methocel) and 2 mpk iv (DMSO). All values are within 25% of the mean. [f] Average of three rhesus macaques dosed at 10 mpk po (0.5% methocel) and 2 mpk iv (DMSO). All values are within 25% of the mean.

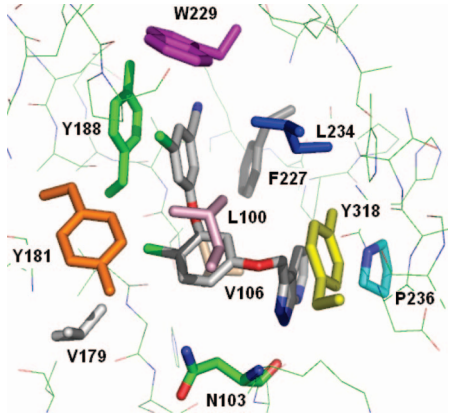

Figure 4. X-ray crystal structure of **8d** (gray) bound in the K103N mutant NNRTI binding site (3.1 angstrom resolution). Key active site residues are labeled in black. Details of the crystallographic studies are provided in ref 10.

of the mutants that were evaluated. Once again, only the Y188L mutant showed notable decreases in antiviral potency, as observed with previous compounds in this series. Cell culture selection experiments with this compound have shown that the Y188L mutation does not appear to arise after treatment with the inhibitor. Under low MOI (multiple of infection) conditions ((1−5) × CIC_{95}), small amounts of Y181C, P236L, and V106A are observed. Under higher MOI conditions at a 200 nM concentration, the V106A mutation is selected after 36 days. Under the highest MOI conditions (1000 nM), no mutations are observed after multiple months of treatment. Crystallographic studies[14] with **8e** were performed in the WT and Y181C mutant enzymes. Figure 5 shows the crystal structure of **8e** bound in the WT active site. The WT crystal structure is essentially identical to the previous structures we have reported in this series, with all previously noted interactions with the active site maintained. Figure 6 shows the crystal structure of **8e** in the Y181C mutant binding site. The binding mode in the Y181C mutant is strikingly similar to that seen in the WT enzyme. The binding of the compound is completely uninfluenced by the mutation of the 181 residue, as the inhibitor does not make any direct interaction with this residue. In total, all crystal structures that we have reported for this series demonstrate remarkably similar binding modes for the inhibitors in the WT and mutant active sites, with only very subtle differences in the central aryl ether conformation and slight movements of the compounds' relative positions in the site noted. It has been proposed in the

Table 3. Antiviral Potency of **8d** and **8e** versus Various Clinically Isolated Mutant Viruses (NL4-3 Isolate)[a]

	IC_{50} (nM)	
mutation	8d	8e
WT	1.5	1.35
G190A	1.8	1.5
G190S	6.8	7.6
L100I	1.1	1.8
K103N	2.5	4.4
Y181C	4.1	5.6
Y188L	900	>1000
V106A	ND	146.7
V179E	ND	5
P236L	ND	4.2
F227L	ND	0.7
K101E/G190A	4.8	10.1
K103N/G190A	4.0	9.6
K103N/P225H	4.8	1.2
K103N/V179E	6.0	9.6
K103N/Y181C	34.1	84
Y181C/G190A	17.1	14.8
K103N/Y181C/G190A	44.7	98.3

[a] Compounds were analyzed in a Monogram Bioscience Phenoscreen assay in the presence of 40% NHS. The IC_{50} is defined as the concentration of compound in cell culture required to block 50% of viral replication. For all compounds, $n = 2$ and the value is geometric mean. All individual values are within ±30% of the mean. Details are provided in ref 11.

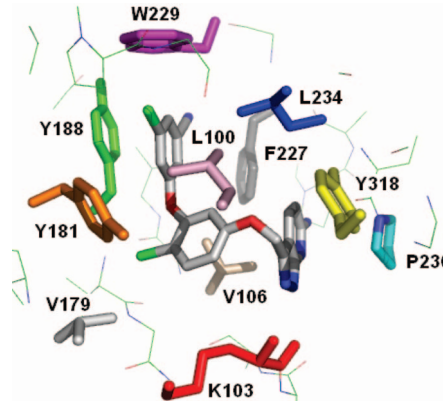

Figure 5. X-ray crystal structure of **8e** (gray) bound in the WT NNRTI binding site (2.6 angstrom resolution). Key active site residues are labeled in black. Details of the crystallographic studies are provided in ref 14.

literature that the ability of NNRTIs to be somewhat conformationally flexible is of critical importance for their broader spectrum antiviral activity.[15] Our results are consistent with this hypothesis; however, the differences in binding modes between the wild-type and mutant enzymes are more subtle. It is likely that the ability of compounds such as **8e** to make direct interactions with the backbone of residue 103 and the ability to avoid direct interaction with Y181 are critical factors in determining the mutant profile of the compounds.

Further preclinical evaluation of **8e** showed the compound to be free of major ancillary activities, including no effects on QTc, heart rate, or blood pressure in a conscious cardiovascular dog model up to 55 μM plasma levels.[16] **8e** demonstrates balanced metabolism in human microsomes via two pathways: oxidation by CYP3A4 on the methylene linker between the central ring and the pyrazolopyridine ring and glucuronidation at N1 of the pyrazolopyridine.[16] In accord with its improved solubility, the compound did not exhibit any difficulties with formulation and had sufficient exposures in safety assessment studies. On the basis of available comparative in-house data, we believe that the overall pharmacokinetic profile of **8e**

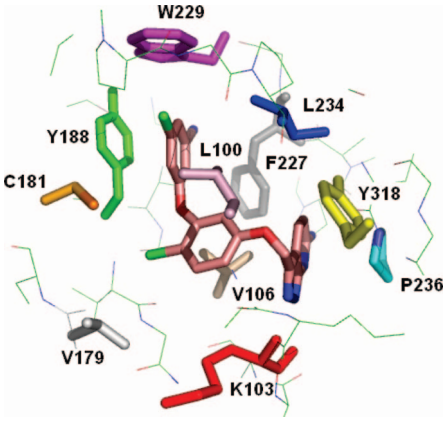

Figure 6. X-ray crystal structure of **8e** (copper) bound in the Y181C mutant NNRTI binding site (2.9 angstrom resolution). Key active site residues are labeled in black. Details of the crystallographic studies are provided in ref 14.

supports development of the compound as a once a day oral agent. As such, the compound was moved forward as a clinical development candidate, labeled as MK-4965.[8] **8e** was shown to have a low potential for drug−drug interactions in preclinical assessments and was clean in genotoxicity assessments, and no major issues were observed in safety assessment studies.[16] On the basis of the results of these studies, **8e** was advanced into phase I clinical trials. Further details of the early clinical studies with **8e**, as well as the pharmacokinetics, formulation, process development, and more extensive SAR studies in this series, will be presented in subsequent publications from our laboratories.

Experimental Section

Silica gel flash chromatography was performed on an Isco Combi-Flash or a Biotage unit using prepacked Isco or Biotage silica cartridges. Reversed phase chromatographic separations were performed on a Gilson unit using Phenomenex Gemini C^{18} columns. ^{1}H NMR spectra were routinely obtained on a 400 MHz Varian FT NMR spectrometer and are referenced versus TMS. NMR solvents used were $CDCl_3$, CD_3OD, or DMSO-d_6 as indicated. Chemical shifts are reported in δ units relative to TMS. HPLC was performed on a Waters Alliance 2695/Micromass ZQ LC/MS system, using a YMC Pro C^{18} 5 μm/120 Å, 3 mm × 50 mm column and a 95:5 to 5:95 A/B gradient (A = 92% water/8% acetonitrile/0.05% TFA; B = 100% acetonitrile with 0.0425% TFA) over 4 or 6 min at a flow rate of 2 mL/min, with UV (215 or 254 nm) and mass spec detection. Aldrich Sure-Seal solvents were used when anhydrous solvents were necessary.

3-Chloro-5-(2-chloro-5-methoxyphenoxy)benzonitrile (4). A mixture of 1.00 g (6.31 mmol) of phenol **2**, 1.28 g (8.20 mmol) of 3-fluoro-5-chlorobenzonitrile **3**, and 2.62 g (18.92 mmol) of anhydrous potassium carbonate in 4 mL of anhydrous 1-methyl-2-pyrrolidinone (NMP) was stirred at 120 °C in a nitrogen atmosphere for 4 h, then stirred at room temperature overnight. The mixture was filtered, and the solids were washed with 25 mL of ethyl acetate. The filtrate was washed with 10 mL of 1 N HCl, 10 mL of 1 N NaOH, and 10 mL of brine. The organic layer was dried over anhydrous $MgSO_4$ and was filtered, and the filtrate was concentrated to an orange oil. The crude oil was purified by flash chromatography over silica gel with 1:1 hexanes/chloroform to give 1.75 g (94%) of the desired product as a white solid. ^{1}H NMR δ (ppm) ($CDCl_3$): 3.81 (3H, s), 6.44 (1H, m), 6.62 (1H, m), 6.78 (1H, m), 7.14 (1H, m), 7.22 (1H, m), 7.37 (1H, m). MS (ES+) *m/z*: [M + H] = 295.

3-Chloro-5-(2-chloro-5-hydroxyphenoxy)benzonitrile (5). A solution of 1.65 g (5.61 mmol) of **4** was dissolved in 15 mL of methylene chloride, and the resulting solution cooled to −15 °C under a nitrogen atmosphere. The solution was treated with 17 mL (17.00 mmol) of 1 M boron tribromide (Aldrich) added as a steady stream. The resulting solution was stirred in the cold for 30 min and allowed to warm to room temperature overnight. The reaction was quenched by adding excess water, and the resulting mixture was extracted with 2 × 50 mL portions of ether. The combined ethereal extracts were washed with 25 mL of brine and dried over anhydrous $MgSO_4$. The mixture was filtered and the filtrate concentrated in vacuo to give 1.55 g (98%) of the desired product as an off-white solid. The material was determined to be of adequate purity (HPLC purity of 96% at 215 nm) to be used without further purification. ^{1}H NMR δ (ppm) ($CDCl_3$): 4.94 (1H, s), 6.62 (1H, m), 6.73 (1H, m), 7.05 (1H, m), 7.16 (1H, m), 7.35 (1H, s), 7.37 (1H, d). MS (ES+) *m/z*: [M + H] = 280.

***tert*-Butyl3-{[4-Chloro-3-(3-chloro-5-cyanophenoxy)phenoxy]methyl}-1*H*-pyrazolo[4,3-*b*]pyridine-1-carboxylate (7a).** To a solution of 83 mg (0.30 mmol) of **5** in 1 mL of anhydrous DMF was added 22 mg (0.33 mmol) of 60% NaH dispersion in oil (Aldrich). The mixture was stirred for 30 min before 93 mg (0.30 mmol) of **6a** was added as a solution in 2 mL of anhydrous DMF. The resulting mixture was stirred for 1 h and was diluted with 10 mL of water and 10 mL of EtOAc. The mixture was extracted with 2 × 20 mL of EtOAc, and the combined organic layers were washed with 4 × 10 mL of water and 2 × 10 mL of brine, dried (anhydrous $MgSO_4$), and concentrated in vacuo to give 160 mg of crude product as a brown oil. The crude product was determined to be 80−90% pure by LC/MS analysis and was used in the next reaction without further purification or characterization.

***tert*-Butyl3-{[4-Chloro-3-(3-chloro-5-cyanophenoxy)phenoxy]methyl}-1*H*-pyrazolo[4,3-*c*]pyridine-1-carboxylate (7b).** A mixture of 40 mg (0.14 mmol) of **5**, 45 mg (0.14 mmol) of **6b**, and 141 mg (0.43 mmol) of Cs_2CO_3 in 3 mL of anhydrous DMF was stirred at ambient temperature overnight or until complete by LC/MS analysis. The mixture was concentrated in vacuo to give 15 mg of crude **7a** as a brown oil. The crude material (80−90% purity by LC/MS analysis) was used as recovered in the next step without further purification.

***tert*-Butyl3-{[4-Chloro-3-(3-chloro-5-cyanophenoxy)phenoxy]methyl}-1*H*-pyrazolo[3,4-*c*]pyridine-1-carboxylate (7c).** In a manner identical to that described above for the preparation of **7b**, from 41 mg (0.15 mmol) of **5**, 46 mg (0.15 mmol) of **6c**, and 144 mg (0.43 mmol) of Cs_2CO_3 was obtained 90 mg of crude **7c** as a brown oil. The crude material (80−90% purity by LC/MS analysis) was used as recovered in the next step without further purification.

***tert*-Butyl3-{[4-Chloro-3-(3-chloro-5-cyanophenoxy)phenoxy]methyl}-1*H*-pyrazolo[3,4-*b*]pyridine-1-carboxylate (7d).** In a manner identical to that described above for the preparation of **7a**, from 80 mg (0.29 mmol) of **5**, 91 mg (0.29 mmol) of **6d**, and 12 mg (0.30 mmol) of 60% NaH dispersion was obtained 150 mg of crude **7d** as a brown oil. The crude material (80−90% purity by LC/MS analysis) was used as recovered in the next step without further purification.

3-Chloro-5-[2-chloro-5-(1*H*-pyrazolo[4,3-*b*]pyridine-3-yl-methoxy)phenoxy]benzonitrile (8a). A solution of 150 mg of crude **7a** was dissolved in 4 mL of TFA and stirred for 30 min. The crude mixture was concentrated in vacuo and was purified using silica gel chromatography (10−60% EtOAc/hexane) to afford 82 mg (67% for two steps) of the title compound as an amorphous white solid. ^{1}H NMR δ (ppm) ($CDCl_3$): 5.58 (2 H, s), 6.93 (1 H, d, J = 3 Hz), 6.97−7.01 (2 H, m), 7.16 (1 H, t, J = 2 Hz), 7.31−7.37 (2 H, m), 7.42 (1 H, dd, J = 9, 5 Hz), 7.95 (1 H, dd, J = 9, 1 Hz), 8.66−8.68 (1 H, m). HRMS (ES+) *m/z*: [M + H] theoretical = 411.0410, obsd = 411.0391. LC purity, >99%; t_R = 2.39 min at 215 nm.

3-Chloro-5-[2-chloro-5-(1*H*-pyrazolo[4,3-*c*]pyridine-3-yl-methoxy)phenoxy]benzonitrile (8b). In a manner identical to that described above for the preparation of **8a**, from 15 mg of crude **7b** was obtained 6 mg (10% for two steps) of the desired product as a white amorphous solid. ^{1}H NMR δ (ppm) (CD_3OD): 5.56 (2 H, s), 6.99 (1 H, d, J = 2.87 Hz), 7.06−7.12 (2 H, m), 7.15 (1 H, t, J = 2 Hz), 7.45−7.52 (2 H, m), 7.56 (1 H, d, J = 6. Hz), 8.33 (1

H, d, $J = 6$ Hz), 9.15 (1 H, s). LC purity, >99%; $t_R = 2.40$ min at 215 nm. HRMS (ES+) *m/z*: [M + H] theoretical = 411.0410, obsd = 411.0426.

3-Chloro-5-[2-chloro-5-(1*H*-pyrazolo[3,4-*c*]pyridine-3-ylmethoxy)-phenoxy]benzonitrile (8c). In a manner identical to that described above for the preparation of **8a**, from 90 mg of crude **7c** was obtained 48 mg (78% for two steps) of the desired product as a white amorphous solid. ^{1}H NMR δ (ppm) (CD_3OD): 5.55 (2 H, s), 6.99 (1 H, d, $J = 2.90$ Hz), 7.06 (1 H, dd, $J = 8.91$, 3.01 Hz), 7.11 (1 H, dd, $J = 6.15$, 2.32 Hz), 7.15 (1 H, t, $J = 2.16$ Hz), 7.47 (1 H, d, $J = 8.89$ Hz), 7.52 (1 H, t, $J = 1.72$ Hz), 7.88 (1 H, dd, $J = 5.72$, 1.40 Hz), 8.23 (1 H, d, $J = 5.71$ Hz), 9.00 (1 H, d, $J = 1.40$ Hz). HRMS (ES+) *m/z*: [M + H] theoretical = 411.0410, observed = 411.0422. LC purity, >99%; $t_R = 2.48$ min at 254 nm.

3-Chloro-5-[2-chloro-5-(1*H*-pyrazolo[3,4-*b*]pyridine-3-ylmethoxy)-phenoxy]benzonitrile (8d). In a manner identical to that described above for the preparation of **8a**, from 150 mg of crude **7d** was obtained crude **8d** as a brown oil. The oil was purified by reversed phase preparative HPLC (Gilson) to give 100 mg (68% for 2 steps) of the TFA salt of the desired product as a fluffy white amorphous powder after lyophilization. ^{1}H NMR δ (ppm) (DMSO-d_6): 5.42 (2H, s), 7.08 (1H, dd, $J = 2$ Hz, 9 Hz), 7.12 (1H, d, $J = 3$ Hz), 7.21 (1H, q), 7.37 (1H, m), 7.46 (1H, m), 7.55 (1H, d, $J = 11$ Hz), 7.80 (1H,m), 8.30 (1H, dd, $J = 1$ Hz, 8 Hz), 8.54 (1H, dd, $J = 1$ Hz, 5 Hz). LC purity, >99%; $t_R = 2.54$ min at 215 nm. HRMS (ES+) *m/z*: [M + H] theoretical = 411.0410, observed = 411.0416.

1-(4-Chloropyridin-3-yl)ethanone (10). A solution of 4.80 mL (33.80 mmol) of diisopropylamine in 20 mL of anhydrous THF cooled to − 78 °C in a nitrogen atmosphere was treated with 21 mL (33.6 mmol) of 1.6 M *n*-BuLi in hexanes (Aldrich). The resulting mixture was warmed to 0 °C for 30 min, recooled to −78C, and was treated dropwise with a solution of 3.20 g (28.30 mmol) of **9** in 10 mL of THF. The mixture was stirred for 2 h and was treated with 3.00 mL (28.30 mmol) of *N*-methoxy-*N*-methylacetamide. The resulting mixture was warmed to room temperature overnight, was poured into water (100 mL), and was extracted with 3 × 50 mL of ethyl acetate. The combined organic layers were washed with brine, dried ($MgSO_4$), filtered, and concentrated in vacuo to provide the crude product. The mixture was purified by silica gel chromatography (0−100% EtOAc/hexane gradient) to afford 1.5 g (34%) of the title compound as an oil. ^{1}H NMR δ (ppm) ($CDCl_3$): 2.64 (3H, s), 7.38 (1H, d), 8.78 (1H, d), 8.80 (1H, s). MS (ES+) *m/z*: [M + H] = 156.3. LC purity, >99%; $t_R = 1.04$ min at 254 nm.

3-Methyl-1*H*-pyrazolo[4,3-*c*]pyridine (11). A solution of 1.50 g (9.60 mmol) of **10** in 15 mL of CH_2Cl_2 was treated with 5.45 g (19.20 mmol) of titanium isopropoxide at room temperature. The resulting mixture was stirred for 30 min and cooled to 0 °C, and 0.96 g (19.20 mmol) of hydrazine hydrate was added. The ice bath was removed and the mixture stirred for 2 h before water (5 mL) was added. The resulting mixture was stirred vigorously for 30 min. The thick precipitate was filtered off and washed with CH_2Cl_2 (100 mL), and the filtrate was concentrated in vacuo. The crude residue was dissolved in 15 mL of ethylene glycol, and the solution was heated at 120 °C for 18 h. The reaction mixture was diluted with an excess of water and was extracted with 100 mL of ethyl acetate. The ethyl acetate extract was washed with 50 mL of brine, dried (anhydrous $MgSO_4$), filtered, and concentrated in vacuo to give 0.60 g (47%) of the crude product as an oil. The material was used as obtained from the reaction without further purification. ^{1}H NMR δ (ppm) ($CDCl_3$): 2.65 (s, 3H), 7.35 (d, $J = 5.8$ Hz, 1H), 8.43 (d, $J = 5.8$ Hz, 1H), 9.08 (s, 1H), 10.10 (bs, 1H). MS (ES+) *m/z*: [M + H] = 134.0. LC purity, >99%; $t_R = 0.37$ min at 254 nm.

***tert*-Butyl 3-Methyl-1*H*-pyrazolo[4,3-*c*]pyridine-1-carboxylate (12).** A suspension of 0.60 g (4.50 mmol) of **11** in 20 mL of acetonitrile was treated with 0.55 g (4.53 mmol) of *N*,*N*-dimethylaminopyridine, 0.66 mL (4.75 mmol) of triethylamine, and 1.18 g (5.43 mmol) of di-*tert*-butyl dicarbonate. The resulting mixture was stirred at room temperature for 1 h and was diluted with an equal volume of brine and extracted with 3 × 25 mL of ethyl acetate. The combined organic extract was washed with 25 mL of brine, dried (anhydrous $MgSO_4$), filtered, and concentrated in vacuo to provide the crude product. The crude product was purified by silica gel chromatography (40−100% EtOAc/hexane gradient) to afford 0.71 g (67%) of the title compound as an oily off-white solid. ^{1}H NMR δ (ppm) ($CDCl_3$): 1.75 (9H, s), 2.68 (3H, 2), 7.95 (1H, d, $J = 6$ Hz), 8.62 (1H, d, $J = 6$ Hz), 9.02 (1H, s). MS (ES+) *m/z*: [M + H − Boc] = 134. LC purity, >99%; $t_R = 1.05$ min at 254 nm.

***tert*-Butyl 3-(Bromomethyl)-1*H*-pyrazolo[4,3-*c*]pyridine-1-carboxylate (6b).** A stirred solution of 500 mg (2.14 mmol) of **12** in 20 mL of carbon tetrachloride was treated with 51 mg (0.21 mmol) of benzoyl peroxide and 400 mg (2.25 mmol) of *N*-bromosuccinimide. The resulting mixture was heated to reflux for 2 h and was cooled to room temperature and concentrated in vacuo. The crude mixture was purified by silica gel chromatography (0−50% ethyl acetate/hexane gradient) to provide 65 mg (20%) of the desired product as an off-white solid. LC purity, >99%; $t_R = 2.01$ min at 254 nM. ^{1}H NMR δ (ppm) ($CDCl_3$): 1.75 (9H, s), 4.80 (3H, s), 7.98 (1H, d, $J = 6$ Hz), 8.65 (1H, d, $J = 6$ Hz 1H), 9.22 (1H, s). MS (ES+) *m/z*: [M + H − Boc] = 212.3. LC purity, >99%; $t_R =$ 2.01 min at 254 nm.

***tert*-Butyl (4-Methylpyridin-3-yl)carbamate (14).** A solution of 5.00 g (108.15 mmol) of **13** in 100 mL of anhydrous THF was treated dropwise with 92.40 mL (92.40 mmol) of 1.0 M NaHMDS in THF (Aldrich). A solution of 9.58 g (43.90 mmol) of di-*tert*-butyl dicarbonate in 30 mL of anhydrous THF was added via a cannula, and the mixture was stirred for 2.5 h at room temperature. The reaction was quenched with excess water and was extracted with 3 × 40 mL of EtOAc. The combined organic layers were washed with brine, dried over $MgSO_4$, filtered, and concentrated in vacuo to provide the crude product as an oil. The mixture was purified by silica gel chromatography (20−60% EtOAc/hexane gradient) to provide 5.95 g (70%) of the desired product as a brown oil/solid. ^{1}H NMR δ (ppm) ($CDCl_3$): 1.52 (9H, s), 2.25 (3H, s), 6.18 (1H, bs), 7.18 (1H, d, $J = 5$ Hz), 8.24 (1H, s, $J = 5$ Hz, 1H), 8.85 (1H, s). MS (ES+) *m/z*: [M + H − Boc] = 153.4. LC purity, >99%; $t_R = 1.09$ min at 215 nm (6 min gradient).

***tert*-Butyl (4-Ethylpyridin-3-yl)carbamate (15).** A solution of 4.00 g (19.20 mmol) of **14** in 80 mL of anhydrous THF was cooled to −78 °C under a nitrogen atmosphere and was treated dropwise with 28.20 mL (48.00 mmol) of 1.7 M *t*-BuLi in pentane (Aldrich). The resulting mixture was stirred at −78 °C for 1 h, was warmed to −20 °C for 45 min, and was recooled to −30 °C. The mixture was treated with a solution 4.08 g (28.80 mmol) of iodomethane in 20 mL of THF (20 mL) added via a cannula. The resulting mixture was maintained between −20 and −30 °C for 45 min. The reaction was quenched with brine, warmed to room temperature, and was extracted with 3 × 40 mL of EtOAc. The combined organic layers were washed with brine, dried (anhydrous $MgSO_4$), filtered, and concentrated in vacuo to provide the crude product as an oil. The crude mixture was purified by silica gel chromatography (10−100% EtOAc/hexanes gradient) to provide 4.15 g (98%) of the desired product as an oil. ^{1}H NMR δ (ppm) ($CDCl_3$): 1.30 (3H, t), 1.54 (9H, s), 2.60 (2H, q), 6.10 (1H, bs), 7.12 (1H, d, $J = 8$ Hz), 8.32 (1H, d, $J = 8$ Hz), 8.88 (1H, s). MS (ES+) *m/z*: [M + H-Boc] = 167.4. LC purity, >99%; $t_R = 1.33$ min at 215 nm (6 min gradient).

4-Ethylpyridin-3-amine (16). A solution of 4.15 g (18.82 mmol) of **15** in 20 mL of TFA was stirred at room temperature for 30 min. The reaction mixture was concentrated in vacuo and the crude oil purified by silica gel chromatography (0−40% MeOH/CH_2Cl_2 gradient) to give 3.03 g (69%) of the TFA salt of the desired product. ^{1}H NMR δ (ppm) (CD_3OD): 1.32 (3H, t), 2.70 (2H, q), 7.60 (1H, d, $J = 8$ Hz), 7.92 (1H, d, $J = 8$ Hz), 7.96 (1H, s). MS (ES+) *m/z*: [M + H] = 123.3. LC purity, >99%; $t_R = 0.42$ min at 215 nm.

3-Methyl-1*H*-pyrazolo[3,4-*c*]pyridine (17). A solution of 550 mg (4.50 mmol) of **16** in H_2O/H_2SO_4 (1:1 volume) cooled to 0 °C was treated with a solution of 341 mg (4.96 mmol) of $NaNO_2$ in 1.4 mL of water. The resulting mixture was stirred at 0 °C for 0.5 h, and the solution was cannulated into 20 mL of 20% aqueous sodium acetate solution. The resulting mixture was stirred for 1.25 h at 0

°C and was extracted with 2 × 25 mL of EtOAc. The combined organic layers were washed with brine, dried ($MgSO_4$), filtered, and concentrated in vacuo to give the crude product. The crude product was purified by silica gel chromatography (0−100% MeOH/CH_2Cl_2 gradient) to give 304 mg (51%) of the desired product as a tan oil/solid. ^{1}H NMR δ (ppm) ($CDCl_3$): 2.62 (3H, s), 7.60 (1H, d, J = 5 Hz), 8.32 (1H, d, J = 5 Hz), 8.98 (1H, s). MS (ES+) m/z: [M + H] = 134.3. LC purity, >93%; t_R = 0.38 min at 254 nm.

***tert*-Butyl 3-Methyl-1*H*-pyrazolo[3,4-*c*]pyridine-1-carboxylate (18).** In a manner identical to that described above for the preparation of **12**, from 95 mg (0.71 mmol) of **17**, 104 μL (0.75 mmol) of TEA, 87 mg (0.71 mmol) of DMAP, and 185 mg (0.85 mmol) of di-*tert*-butyl dicarbonate (185 mg, 0.85 mmol) was obtained 97 mg (59%) of the desired product. ^{1}H NMR δ (ppm) (CD_3OD): 1.75 (9H, s), 2.64 (3H, s), 7.85 (1H, d, J = 5 Hz), 8.48 (1H, d, J = 5 Hz), 9.40 (1H, s). MS (ES+) m/z: [M + H − Boc] = 134.3. LC purity, >99%; t_R = 1.30 min at 215 nm.

***tert*-Butyl 3-(Bromomethyl)-1*H*-pyrazolo[3,4-*c*]pyridine-1-carboxylate (6c).** In a manner identical to that described above for the preparation of compound **12**, from 97 mg (0.42 mmol) of **18**, 7 mg (0.44 mmol) of NBS, and 10 mg (0.04 mmol) of benzoyl peroxide was obtained 47 mg (36%) of the desired product as an off-white solid. ^{1}H NMR δ (ppm) ($CDCl_3$): 1.77 (9H, s), 4.80 (2H, 2), 7.75 (1H, dd, J = 1, 5 Hz), 8.55 (1 h, d, J = 5 Hz), 9.50 (1H, s). MS (ES+) m/z: [M + H − Boc] = 212.2. LC purity, >99%; t_R = 1.77 min at 254 nm.

1-(2,6-Difluoropyridin-3-yl)ethanone (20). A solution of 32.70 g (323.00 mmol) of diisopropylamine in 550 mL of anhydrous THF was cooled to −78 °C under a nitrogen atmosphere and was treated with 200.00 mL (318.00 mmol) of 1.6 M *n*-BuLi in hexanes (Aldrich). The resulting solution naturally warmed to −20 °C and was maintained at −20 °C for 1.5 h. The solution was recooled to −78 °C, and a solution of 31.00 g (269.00 mmol) of **19** in 100 mL of anhydrous THF was added dropwise. The reaction was continued with stirring for 2 h at −78 °C and was treated with a solution of 28.60 mL (269.00 mmol) of *N*-methoxy-*N*-methylacetamide in 20 mL of THF added via a cannula. The resulting solution was warmed to ambient temperature overnight and was quenched with excess brine solution. The mixture was extracted with 3 × 100 mL of ethyl acetate, and the combined organic layers were washed with 100 mL of water and 2 × 100 mL of brine, dried (anhydrous $MgSO_4$), filtered, and concentrated in vacuo. The crude oil was purified via silica gel chromatography (0−40% EtOAc/hexane gradient) to afford 10.70 g (25%) of the desired product a clear, pale-yellow oil. ^{1}H NMR δ (ppm) ($CDCl_3$): 2.68 (3H, s), 6.95 (1H, d, J = 6 Hz), 8.50 (1H, m). MS (ES+)m/z: [M + H] = 158.0. LC purity, >99%; t_R = 1.40 min at 254 nm.

6-Fluoro-3-methyl-1*H*-pyrazolo[3,4-*b*]pyridine (21). A solution of 29.00 g (185.00 mmol) of **20** in 450 mL of CH_2Cl_2 was treated with 108.00 mL (369.00 mmol) of titanium(IV) isopropoxide at room temperature. The resulting mixture was stirred for 15 min, and 17.96 mL (369.00 mmol) of hydrazine hydrate was added. Stirring continued for an additional 1.5 h. Water (40 mL) was added, and the resulting thick mixture was stirred vigorously for 20 min. The reaction mixture was filtered, and the solids were washed with 100 mL of CH_2Cl_2. The filtrate was concentrated in vacuo to provide the crude hydrazone intermediate as an oil. The crude hydrazone was dissolved in 150 mL of ethanol, and the solution was heated at 80 °C for 24 h. The mixture was cooled and concentrated in vacuo to provide 26.50 g (95%) of crude product as an oil. The crude product was used in the next reaction without further purification. ^{1}H NMR δ (ppm) ($CDCl_3$): 2.56 (3H, s), 6.78 (1H, d, J = 8 Hz), 8.08 (1H, t, J = 8 Hz). MS (ES+) m/z: [M + H] = 152.0. LC purity, 85%; t_R = 1.19 min at 254 nm.

***tert*-Butyl 6-Fluoro-3-methyl-1*H*-pyrazolo[3,4-*b*]pyridine-1-carboxylate (22).** A solution of 23.65 g (156.00 mmol) of **21** in 400 mL of acetonitrile was treated with 19.12 g (156.00 mmol) of DMAP and 22.90 mL (164.00 mmol) of TEA. The resulting solution was stirred for 5 min before a solution of 43.60 mL (188.00 mmol) of di-*tert*-butyl dicarbonate in 100 mL of acetonitrile was added. The mixture was stirred at room temperature for 30 min, was quenched with brine, and was extracted with 2 × 150 mL of EtOAc. The combined organic extracts were washed with 2 × 100 mL of water and 2 × 100 mL of brine, dried (anhydrous $MgSO_4$), and filtered, and the filtrate was concentrated in vacuo. The crude oil was purified by silica gel chromatography (25% EtOAc/hexane) to provide the 25 g (64%) of the desired compound as a clear oil/solid. ^{1}H NMR δ (ppm) ($CDCl_3$): 1.74 (9H, s), 2.60 (3H, s), 6.95 (1H, d, J = 8 Hz), 8.08 (1H, t, J = 8 Hz). HRMS (ES+) m/z: [M + H] theoretical = 252.1143, obsd = 252.1141. LC purity, >99%; t_R = 1.96 min at 254 nm.

***tert*-Butyl 3-(Bromomethyl)-6-fluoro-1*H*-pyrazolo[3,4-*b*]pyridine-1-carboxylate (23).** A solution of 25.00 g (99.00 mmol) of **22** in 500 mL of carbon tetrachloride was treated with 19.48 g (109.00 mmol) of NBS and 2.41 g (9.95 mmol) of benzoyl peroxide. The resulting mixture was heated at reflux for 6 h. The mixture was cooled to room temperature and filtered, and the filtrate was concentrated in vacuo to yield the crude product as an oil. The mixture was purified by silica gel chromatography (10−25% EtOAc/hexane gradient) to give 21.00 g (64%) of the desired product as an off-white/pale-yellow solid that was stored in the freezer. ^{1}H NMR δ (ppm) ($CDCl_3$): 1.75 (9H, s), 4.75 (2H, s), 7.00 (1H, d, J = 8 Hz), 8.30 (1H, t, J = 8 Hz). HRMS (ES+) m/z: [M + Na] theoretical = 352.0067, obsd = 352.0079. LC purity, >99%; t_R = 1.94 min at 254 nm.

3-Chloro-5-{2-chloro-5-[(6-fluoro-1*H*-pyrazolo[3,4-*b*]pyridin-3-yl)methoxy]phenoxy}benzonitrile (24). A solution of 2.97 g (10.68 mmol) of **5** in 15 mL of 1-methyl-2-pyrrolidinone was treated with 6.58 g (20.30 mmol) of Cs_2CO_3. The mixture was stirred for 20 min, and a solution of 3.34 g (10.15 mmol) of **23** in 20 mL of 1-methyl-2-pyrrolidinone was added. The resulting mixture was stirred for 1.5 h and was poured into 2.5 L of ice−water. The mixture was extracted with 3 × 150 mL EtOAc, and the combined organic layers were washed with 4 × 100 mL of water and 2 × 100 mL of brine. The organic layer was dried ($MgSO_4$) and filtered, and the filtrate was concentrated in vacuo to give the crude product as a brown oil. The crude product was purified by silica gel chromatography (10−60% EtOAc/hexanes gradient) to afford 4.60 g (86%) of the desired product as an oil/solid. ^{1}H NMR δ (ppm) ($CDCl_3$): 1.73 (9H, s), 5.42 (2H, s), 6.80 (1H, m), 6.93−6.98 (2H, m), 7.01 (1H, m), 7.13 (1H, m), 7.36 (1H, m), 7.42 (1H, d, J = 8 Hz), 8.28 (1H, t, J = 8 Hz). HRMS (ES+) m/z: [M + H] theoretical = 546.1106, obsd = 546.1128. LC purity, >99%; t_R = 3.73 min at 254 nm.

3-Chloro-5-[2-chloro-5-({6-[(4-methoxybenzyl)amino]-1*H*-pyrazolo[3,4-*b*]pyridin-3-yl}methoxy)phenoxy]benzonitrile (25). A solution of 200 mg (0.30 mmol) of **24** in 2.50 mL of 1-methyl-2-pyrrolidinone was treated with 410 mg (3.00 mmol) of *p*-methoxybenzylamine, and the resulting solution was heated at 95 °C for 18 h. The mixture was cooled to room temperature and was diluted with 5 mL of 1/1 brine/H_2O solution. The resulting mixture was extracted with 3 × 25 mL of ethyl acetate, and the combined extracts were washed with 4 × 25 mL of water and 2 × 25 mL of brine. The extract was dried (anhydrous $MgSO_4$) and filtered, and the filtrate was concentrated in vacuo to give the crude product as a brown oil. The crude material was purified by silica gel chromatography (20−100% EtOAc/hexane gradient) to provide 51 mg (31%) of the desired product as an oil. ^{1}H NMR δ (ppm) ($CDCl_3$): 3.80 (3H, s), 4.58 (2H, s), 4.98 (1H, m), 5.30 (2H, s), 6.30 (1H, d,, J = 8.4 Hz), 6.82 (1H, m), 6.85 (2H, d, J = 8.4 Hz), 6.92 (1H, d, J = 8.4 Hz), 7.00 (1H, s), 7.10 (1H, s), 7.25−7.38 (4H, m), 7.78 (1H, d, J = 8.4 Hz). MS (ES+)m/z: [M + H] = 546.3. LC purity, >99%; t_R = 2.51 min at 254 nm.

3-{5-[(6-Amino-1*H*-pyrazolo[3,4-*b*]pyridin-3-yl)methoxy]-2-chlorophenoxy}-5-chlorobenzonitrile (8e). A solution of 51 mg (0.09 mmol) of **25** in 5 mL of TFA was heated at 60 °C for 7 h. The reaction mixture was concentrated in vacuo and purified using reverse phase chromatography (Gilson) to afford 15 mg (30%) of the TFA salt of the desired compound as a fluffy white amorphous solid after lyophilization. ^{1}H NMR δ (ppm) (CD_3OD): 5.40 (2H, s), 6.58 (1H, d, J = 9 Hz), 6.93 (1H, d, J = 3 Hz), 7.04 (1H, dd,

$J = 3, 9$ Hz), 7.11 (1H, m), 7.15 (1H, m), 7.46 (1H, d, $J = 9$ Hz), 7.52 (1H,m), 8.10 (1H, d, $J = 9$ Hz). HRMS (ES+) *m/z*: [M + H] theoretical = 426.0519, obsd = 426.0519. LC purity, >99%; t_R = 1.93 min at 254 nm.

Acknowledgment. The authors thank Dr. Charles Ross and Joan Murphy for high resolution mass spectral data. We also thank Dr. Sandor Varga for NMR support.

References

(1) Demeter, L. M.; Doamaoal, R. A. Structural and biochemical effects of HIV-1 virus mutants resistant to NNRTIs. *Int. J. Biochem. Cell Biol.* **2004**, *36*, 1735–1751.

(2) Tarby, C. M. Recent advances in the development of next generation NNRTIs. *Curr. Top. Med. Chem.* **2004**, *4*, 1045–1057.

(3) http://www.tibotec.com/bgdisplay.jhtml?itemname=HIV_tmc125.

(4) Tucker, T. J.; Saggar, S.; Sisko, J. T.; Tynebor, R. M.; Williams, T. M.; Felock, P. J.; Flynn, J. A.; Lai, M.-T.; Liang, Y.; McGaughey, G.; Liu, M.; Miller, M.; Moyer, G.; Munshi, V.; Perlow-Poehnelt, R.; Prasad, S.; Sanchez, R.; Torrent, M.; Vacca, J. P.; Wan, B.-L.; Yan, Y. The design and synthesis of diaryl ether second generation NNRTIs with enhanced potency versus key clinical mutations. *Bioorg. Med. Chem. Lett.* **2008**, *18*, 2959–2966.

(5) Henke, B. R.; Aquino, C. J.; Birkemo, L. S.; Croom, D. K., Jr.; Ervin, G. N.; Grizzle, M. K.; Hirst, G. C.; James, M. K.; Johnson, M. F.; Queen, K. L.; Sherrill, R. G.; Sugg, E. E.; Suh, E. M.; Szewczyk, J. W.; Unwalla, R. J.; Yingling, J.; Willson, T. M. Optimization of 3-(1*H*-Indazol-3-ylmethyl)-1,5- benzodiazepines as potent, orally active CCK-A agonists. *J. Med. Chem.* **1997**, *40* (17), 2706–2725.

(6) Zhang, N.; Tomizawa, M.; Casida, J. E. Structural features of azidopyridinyl neonicotinoid probes conferring high affinity and selectivity for mammalian α4*β*2 and *Drosophila* nicotinic receptors. *J. Med. Chem.* **2002**, *45* (13), 2832–2840.

(7) Marakos, P.; Pouli, N.; Wise, D. S.; Townsend, L. B. A new and facile method for the preparation of 3-substituted pyrazolo[3,4-*c*]pyridines. *Synlett* **1997**, *05*, 561–563.

(8) Full experimental protocols for the HIV-1 RT Polymerase SPA assay are described in the following patent application: Saggar, S. A.; Sisko, J. T.; Tucker, T. J.; Tynebor, R. M.; Su, D.-S.; Anthony, N. J. Preparation of Heterocyclic Phenoxy Compounds as HIV Reverse Transcriptase Inhibitors. U.S. Patent Appl. US 2007/021442 A1, 2007.

(9) Vacca, J. P.; Dorsey, B. D.; Schleif, W. A.; Levin, R. B.; McDaniel, S. L.; Darke, P. D.; Zugay, J.; Quintero, J. C.; Blahy, O. M.; Roth, E.; Sardana, V. V.; Schlabac, A. J.; Graham, P. I.; Condra, J. H.; Gotlib, L.; Holloway, M. K.; Lin, J.; Chen, I.-W.; Vastag, K.; Ostovic, D.; Anderson, P. S.; Emini, E. E.; Huff, J. R. L-735,524: an orally bioavailable human immunodeficiency virus type 1 protease inhibitor. *Proc. Natl. Acad. Sci. U.S.A.* **1994**, *91*, 4096–4100.

(10) The X-ray diffraction data of the K103N RT and inhibitor **8d** complex crystal (Figure 4) were collected at 3.15 Å resolution with R_{sym} of 0.085 and 100% completeness. The structure was refined to an *R*-factor of 0.184. The structure has been deposited in the PDB; PDB code is 3DRS.

(11) The compound was evaluated in a Monogram Bioscience PhenoSense assay versus a panel of clinically derived RT mutants in the presence of 40% normal human serum. Values are the average of two determinations. Assays were performed by Monogram Bioscience, South San Francisco, CA. Details of the assay protocols are available at http://www.monogramhiv.com/assays/hcp/phenoHIVTechnology.aspx.

(12) Dykes, C.; Demeter, L. M. Y188H, Which Is a Potential Intermediate between Wild-Type (WT) and Y188L, Has Markedly Reduced Replication Efficiency. *Abstracts of Papers*, 14th Conference on Retroviruses and Opportunistic Infections, Los Angeles, CA, Feb 25−28, 2007; Poster 633.

(13) Compound **8e** was placed in the NNRTI binding pocket based on prior knowledge of related compounds in NNRTI crystal structures. Approximately 30 conformations of each compound was generated using two algorithms: a distance geometry (ref (a)) and a knowledge based (ref (b)) method. All conformations were then subjected to energy minimization using the distance dependent dielectric constant of **2** and applying the MMFFs force field (ref (c)). All figures were created in PyMol (ref (d)). Modeling discussion references: (a) Crippen, C. M.; Havel, T. F. In *Distance Geometry and Molecular Conformation*; Bawden, E., Ed.; Research Studies Press: Wiley, NY, 1988. (b) Kuszewski, J.; Nilges, M.; Brunger, A. T. Sampling and efficiency of metric matrix distance geometry: a novel partial metrization algorithm. *J. Biomol. NMR* **1992**, *2*, 33–56. (c) Feuston, B. P.; Miller, M. D.; Culberson, J. C.; Nachbar, R. B.; Kearsley, S. L. Comparison of knowledge-based and distance geometry approaches for generation of molecular conformations. *J. Chem. Inf. Comput. Sci.* **2001**, *41*, 754–763. (d) Halgren, T. A. Merck molecular force field. I. Basis, form, scope, parameterization, and performance of MMFF94. *J. Comput. Chem.* **1996**, *17*, 490, 520, 553, and 616. (e) Halgren, T. A.; Nachbar, R. B. Merck molecular force field. IV. Conformational energies and geometries for MMFF94. *J. Comput. Chem.* **1996**, *17*, 587–615. (f) PyMol, version 99, distributed by DeLano Scientific LLC, was utilized to generate all images.

(14) The X-ray diffraction data of the wild type RT and inhibitor **8e** complex crystal (Figure 5) was collected at 2.6 Å resolution with R_{sym} of 0.057 and 100% completeness. The structure was refined to an *R*-factor of 0.187. The structure has been deposited in the PDB; PDB code is 3DRP. The X-ray diffraction data of the Y181C RT and inhibitor **8e** complex crystal (Figure 6) was collected at 2.9 Å resolution with R_{sym} of 0.067 and 100% completeness. The structure was refined to an *R*-factor of 0.183. The structure has been deposited in the PDB; PDB code is 3DRR.

(15) Das, K.; Clark, A. D., Jr.; Lewi, P. J.; Heeres, J.; De Jonge, M. R.; Koymans, L. M. H.; Vinkers, H. M.; Daeyaert, F.; Ludovici, D. W.; Kukla, M. J.; De Corte, B.; Kavash, R. W.; Ho, C. Y.; Ye, H.; Lichtenstein, M. A.; Andries, K.; Pauwels, R.; De Bethune, M.-P.; Boyer, P. L.; Clark, P.; Hughes, S. H.; Janssen, P. A. J.; Arnold, E. Roles of conformational and positional adaptability in structure-based design of TMC125-R165335 (etravirine) and related non-nucleoside reverse transcriptase inhibitors that are highly potent and effective against wild-type and drug-resistant HIV-1 variants. *J. Med. Chem.* **2004**, *47* (10), 2550–2560.

(16) Unpublished data, Merck Research Laboratories.

JM800856C